Journal of Applied Physics ARTICLE scitation.org/journal/jap

Determination of single crystal elastic moduli of KTb_3F_{10} by resonant ultrasound spectroscopy

Cite as: J. Appl. Phys. **128**, 165104 (2020); doi: 10.1063/5.0024723
Submitted: 11 August 2020 · Accepted: 6 October 2020 ·
Published Online: 26 October 2020 · Corrected: 28 October 2020

Ashiwini Balodhi,[1] Kelvin Chang,[2] Kevin T. Stevens,[2] Sunil K. Chakrapani,[3] Susan M. Ennaceur,[4] Albert Migliori,[5] and Alexandra Zevalkink[1,a)]

AFFILIATIONS

[1]Department of Chemical Engineering and Materials Science, Michigan State University, East Lansing, Michigan 48824, USA
[2]Northrop Grumman SYNOPTICS, Charlotte, North Carolina 28273, USA
[3]Department of Electrical and Computer Engineering, Michigan State University, East Lansing, Michigan 48824, USA
[4]Alamo Creek Engineering, 13 Alamo Creek Drive, Santa Fe, New Mexico 87545, USA
[5]Los Alamos National Laboratory, Los Alamos, New Mexico 87545, USA

[a)]**Author to whom correspondence should be addressed:** alexzev@msu.edu

ABSTRACT

KTb_3F_{10} (KTF) has been developed in recent years as a candidate Faraday rotator material because of its cubic symmetry, high figures of merit, and low absorption coefficient. While considerable efforts have focused on crystal growth and optical properties, investigations of fundamental thermodynamic behavior of KTF have been limited. Here, we report elastic moduli C_{11}, C_{12}, and C_{44} of single crystalline KTF measured by resonant ultrasound spectroscopy from 280 K up to 300 K and the obtained temperature derivatives of each modulus. We additionally report the single crystal elastic moduli of the rare-earth garnet $Y_3Al_5O_{12}$ (YAG), yielding results that agree well with the prior literature. We found $C_{11} = 135.62$ GPa, $C_{12} = 58.11$ GPa, and $C_{44} = 44.81$ GPa for KTF and $C_{11} = 332.43$ GPa, $C_{12} = 109.58$ GPa, and $C_{44} = 114.81$ GPa for YAG at room temperature. The present results have been compared with previous experimental and theoretical results and with common oxide and fluoride optical materials, revealing the relative softness of KTF. The low elastic moduli of KTF are, in turn, responsible for its low thermal conductivity and low Debye frequency compared to other laser host materials.

I. INTRODUCTION

Faraday rotation is a magneto-optical phenomenon by which the polarization of incident light is rotated in the presence of a stationary magnetic field. Faraday rotator materials are the essential component of Faraday isolators, which allow light to propagate almost unimpeded in the forward direction and protects the laser from back-reflected radiation. They are used in the construction of fast modulators, optical switches, and isolators in laser systems and as a nonreciprocal element in laser gyroscopes.[1–3] Today, the most common host mediums for Faraday materials (a magneto active) are rare-earth garnets $Tb_3Ga_5O_{12}$ (TGG) and $Tb_3Al_5O_{12}$ (TAG), but their thermal lensing and depolarization effects become limiting factors at high laser powers.[4–6] To overcome these drawbacks, considerable effort has been made to develop alternative materials.[7–9] Weber *et al.* recently reported the alkali fluoride KTb_3F_{10} (KTF) as a promising candidate that is better suited for high power laser applications than TGG.[10] KTF combines a low IR absorption constant of ∼0.02%/cm, high optical transparency, a high Verdet constant of ∼36 rad/T m, and a nonlinear low refractive index of $\sim 1 \times 10^{-19}$, which leads to an impressive figure of merit for Faraday rotation in the 500–1600 nm wavelength range.[10–14]

While considerable efforts have focused on optimizing the crystal growth and optical properties of KTF,[13,14] investigations of its thermodynamic behavior have been limited. In particular, the elastic moduli of KTF—one of the most fundamental properties of a material—have not been previously reported. Accurate values of elastic moduli are necessary to model diverse material properties, including thermal conductivity, electrical conductivity (electron–phonon coupling), and mechanical performance.[15] Further, the optical transparency of a material in the infrared range is dependent on the phonon energies and the elastic moduli can be used to

estimate a material's maximum phonon frequency (i.e., the Debye frequency).[16,17] Although elastic moduli are of fundamental importance, the total number of crystalline compounds for which the complete elastic tensor has been experimentally characterized is limited to several hundred. This is primarily because of the difficulty of growing and orienting high-quality single crystals for accurate measurements. For this reason, new experimental reports of elastic tensors are valuable.[18,19]

In the present study, we report the complete elastic tensor of single crystal KTF measured as a function of temperature using resonant ultrasound spectroscopy (RUS). We also report the temperature-dependent elastic moduli of the classical optical material, $Y_3Al_5O_{12}$ (YAG), measured using the same method.[20–23] Since both KTF [space group—*Fm3m* (#225)] and YAG [space group—*Ia3d* (#230)] form cubic structures,[10,20] three independent elastic tensor components, C_{11}, C_{12}, and C_{44}, are sufficient to describe their elastic behavior.[19] By comparing the experimental elastic moduli across a large number of optical materials, we are further able to shed light on the relationship between the elastic behavior and functional properties, including thermal conductivity and optical absorption.

II. EXPERIMENTAL DETAILS

Resonant ultrasound spectroscopy (RUS) and pulse-echo ultrasound and experiments were performed on colorless high-quality single crystals of KTF and YAG. Samples were cut from larger single crystal boules grown by Northrop Grumman SYNOPTICS using the Czochralski technique as described in Ref. 9. For the present study, crystals were cut and polished to yield rectangular parallelepipeds with faces oriented along the {100} family of surfaces. The dimensions and geometric density of each crystal are listed in Table 1 in the supplementary material. Within the experimental error, the measured geometric densities are equal to the theoretical densities (x-ray density) of 5.82 g/cm^3 for KTF and 4.55 g/cm^3 for YAG.

Traditional pulse-echo ultrasound measurements were used to obtain initial values for two of the three elastic moduli, the details of which can be found in Section 1 in the supplementary material. These velocity measurements provided the initial guess of elastic constant for RUS measurements. RUS is a nondestructive ultrasonic technique used to measure elastic properties (vibrational eigenmodes) of solid samples.[24–26] Obtaining accurate elastic tensor coefficients C_{ij} requires the measurement of a large number of mechanical resonant frequencies in a sample of known crystallographic orientation and shape. The room temperature RUS experiments were performed using the commercial system described in Ref. 26. Temperature-dependent data from 295 K to 345 K were collected with an RTC004 system from Alamo Creek Engineering using a thermoelectric heater/cooler. The RTC004 can control the temperature with stability of 10 mK, allowing for accurate determination of the slope of the elastic moduli with temperature. Samples were mounted with diagonally opposite corners contacting the two piezoelectric transducers (shown in Fig. 1 in the supplementary material) to approximate free boundary conditions with excitation frequencies from 150 to 549 KHz.

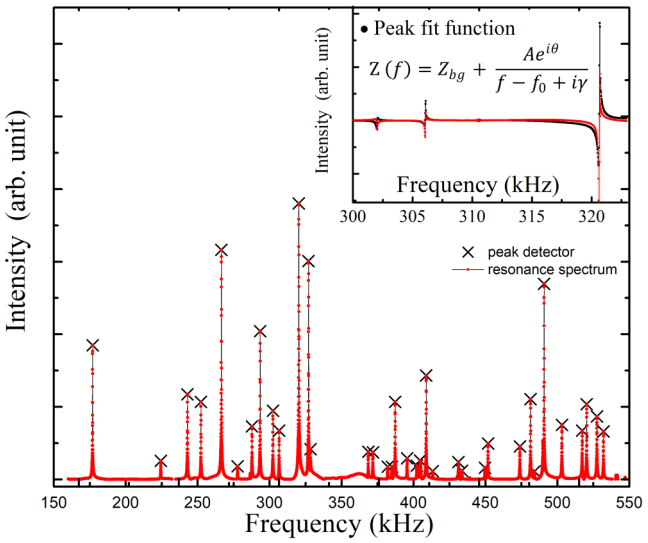

FIG. 1. Room temperature RUS spectrum vs frequency for KTF#2 is shown in red. Black x's indicate the resonant peaks used to determine the elastic moduli. Inset: (black) peak fitting of RUS spectrum (red) by using the peak fit function described in Ref. 26.

After collecting the resonance spectrum via two transducers, the resonance detector attempts to fit individual and overlapping resonances to a complex Lorentzian function: $Z(f) = \frac{Ae^{i\theta}}{f - f_0 + iB} + Z_{bg}$, where f_0 is the center frequency, B is the resonance half-width, A is the amplitude, θ is the phase, and Z_{bg} is the background signal. The inset of Fig. 1 shows a representative individual peak fit. The results of the fit for each resonance, including its width, center frequency, relative phase, and amplitude are recorded and further compared with the theoretical model by using a commercial software rectangular parallelepiped resonator (RPR) code.[26] By minimizing the deviation (percentage error) between calculated and experimentally measured resonance, RPR code provides the percentage error for each mode the elastic moduli C_{ij}.

III. RESULTS AND DISCUSSION

A. Determination of room temperature elastic moduli

The elastic moduli of two KTF crystals and two YAG crystals were measured as part of this study. Both compounds have cubic symmetry,[10,20] meaning that three tensor elements (C_{11}, C_{44}, and C_{12}) can be used to completely describe their elastic properties. Figure 1 shows a representative room temperature RUS spectrum and the peak positions from 150 to 540 KHz for one of the KTF crystals. At room temperature, 30 modes (far more than the minimum required to determine the three elastic moduli) were used in the fitting technique with a percentage error of $\leq$0.28%. This percentage error between measured and calculated resonances is generated for each resonance and can be found in the data provided in the fourth column of Sections 6 and 7 in the supplementary material.

This difference between measured and computed modes is caused by deviations in geometry, crystallinity, and crystallographic orientation from those assumed in the model. The minimal error in the present measurements supports the high-quality cut and single crystalline nature of the specimens used in this study. The inset of Fig. 1 shows the peak fitting of RUS data by using the Lorentzian function.[26]

The results for the two KTF and two YAG crystals are summarized in Table I, along with previously published experimental results of YAG. The results for YAG samples were consistent with the reported values, which were measured on single crystalline YAG sample using Brillouin-light-scattering spectroscopy and phase-cancellation techniques,[20–23] confirming the accuracy of the present method.

The Born mechanical stability criteria for cubic symmetry, $(C_{11} - C_{12}) > 0$, $C_{11} > 0$, $C_{44} > 0$, $(C_{11} + 2C_{12}) > 0$ given in Refs. 27 and 28, were found to be met for both KTF and YAG crystals. Further, we calculated the directionally averaged shear modulus G, bulk modulus B, and Young's modulus Y for KTF and YAG crystals by using the Voigt–Reuss approximation[28–31] and listed them in Table I. The related equations used for these listed parameters in Table I are provided in Section 4 in the supplementary material. A comparison of the moduli of KTF and YAG shows that KTF is a significantly softer material in all respects: it is softer with respect to resistance to volume change under isostatic pressure (B) and with respect to resistance to uniaxial stress (Y) and shear stress (G).[32]

B. Temperature-dependence of the elastic moduli

In the present study, we have measured the temperature evolution of the elastic tensor components C_{11}, C_{12}, and C_{44} for all four KTF and YAG samples. Results are shown in Fig. 2. To obtain an accurate slope in light of the small amount of variation over the measured temperature range, we fit the RUS spectra at each temperature with the same number of modes, such that if a mode is missed in one scan, it must be weighted zero for all other scans, even if it is present (refer to column 5 for mode 9 in Section 6 in the supplementary material). Also, if the error jumps substantially at some temperature for a particular mode, then that mode is likely in the linear interaction regime and must be weighted zero for all temperatures. The fitted results for each analysis are listed in Section 7 in the supplementary material.

In the investigated temperature interval for all samples, the elastic moduli vary linearly with temperature with a negative temperature derivative. As shown in Fig. 2, the smooth decrease of the elastic moduli with temperature indicates the absence of any phase transition in the measured temperature range of KTF and YAG samples.

Generally, increasing temperature leads to thermal expansion and lower elastic moduli. With decreasing temperature, the model developed by Varshni[33] predicts that the elastic moduli will stiffen linearly, before eventually becoming a constant at low liquid helium temperatures. The slope of the bulk modulus vs temperature (dB/dT) in the linear region is related to the Grüneisen parameter (γ), which describes the degree of anharmonicity in the bonding of the solid[34] as

$$\frac{\partial B}{\partial T} = -\frac{3K_B\gamma(\gamma+1)}{V_a}. \quad (1)$$

Here, K_B, γ, and V_a denote Boltzmann's constant, the Grüneisen parameter, and the atomic volume, respectively. We found $\gamma = 1.64$ for YAG and 1.4 for KTF crystal. The smaller Grüneisen parameter is a result of the lower slope of the moduli of KTF with respect to temperature as compared to YAG. We have also performed a comparison of elastic tensor components C_{ij} vs temperature between our YAG results and a previous report from Alton and Barlow,[22] shown in Section 5 in the supplementary material. The temperature derivatives agree reasonably well, with the greatest disparity in dC_{44}/dT (-0.43 in the current study vs -0.57 in Ref. 22).

C. Origin and significance of soft elastic moduli in KTF

A survey of elastic moduli of various crystalline optical materials reveals that, when compared with other fluorides, the low elastic moduli of KTF are not unusual. Figure 3 compares the bulk moduli vs average bond length of different laser host materials at room temperature, including cubic as well as some tetragonal laser host materials (e.g., $PbTiO_3$, $CaMo_4$, $SrMoO_4$, and $MgAl_2O_4$[42–45]). In general, compounds containing larger atoms, therefore having longer bonds, tend to exhibit lower elastic moduli. However, as can be seen in Fig. 3, there is a clear disparity between the stiffer oxides (blue circles) and softer fluorides (red circles), that cannot be explained by differences in the bond length. In general, the weaker

TABLE I. Measured values of the single crystal elastic moduli (C_{ij}), averaged bulk modulus (B), shear modulus (G), Young's modulus (Y), average sound (v_a), and Debye temperature (Θ_D) for KTF and YAG samples in the current study and literature data for YAG.

Sample	C_{11} (GPa)	C_{44} (GPa)	C_{12} (GPa)	B (GPa)	G (GPa)	Y (GPa)	v_a (m/s)	Θ_D (K)	Reference
KTF#1	135.62	44.81	58.11	83.95	42.28	108.61	2982	357.91	
KTF#2	137.99	45.42	59.35	85.57	42.87	110.21	3003	360.49	
YAG#1	336.08	115.28	112.90	187.29	111.29	279.29	5448	719.21	
YAG#2	332.43	114.81	109.58	183.86	111.86	278.09	5442	718.73	
YAG	339	116	114	…	…	…	…	…	20
YAG	333	114	114	…	…	…	…	…	22
YAG	334	115.1	111.2		…	…	…	…	23

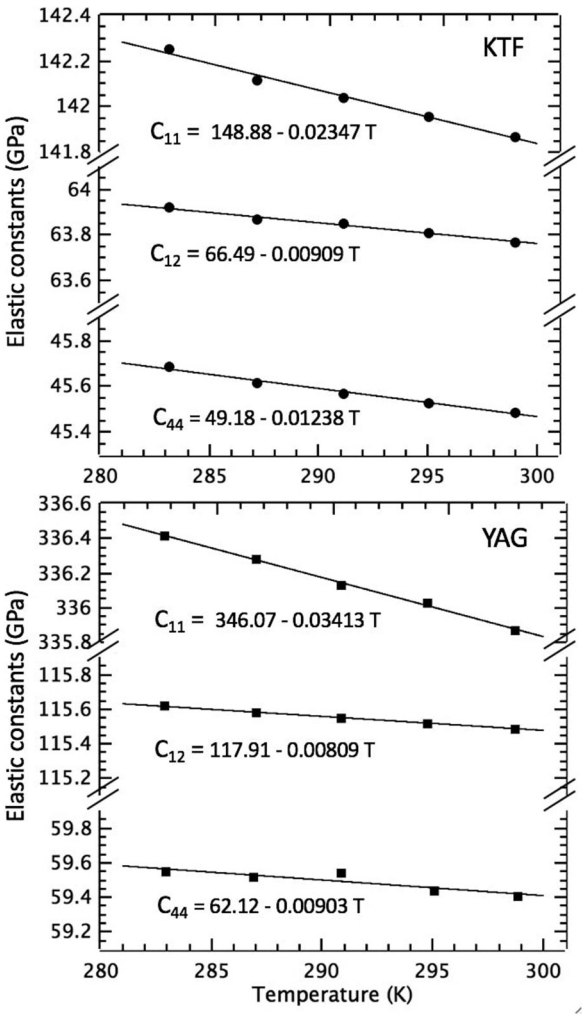

FIG. 2. Elastic moduli C_{11}, C_{12}, and C_{44} vs temperature for the KTF#2 and YAG#2 crystals.

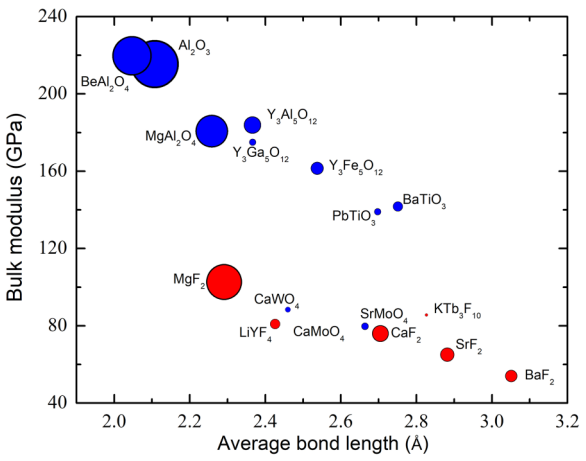

FIG. 3. Bulk modulus vs average bond length of different laser host materials. The bubble size corresponds to the experimental thermal conductivity of the materials, which are listed in the supplementary material. Oxides are shown in blue and fluorides in red.

bonding in fluoride compounds is considered to be the result of their ionic (and thus less directional) bonding character as well as the low field strength associated with the F^- oxidation state.[38,39]

Weaker bonding in fluorides has several consequences; in addition to being important for mechanical performance, the elastic stiffness of optical materials is a predictor of functional properties including thermal conductivity and optical absorption. The general trend between the elastic properties and thermal conductivity is illustrated by the size of the symbols in Fig. 3, which indicates the experimental room temperature thermal conductivity, κ. Note that the reported values of thermal conductivity, bulk modulus, and average bond lengths can be found in Section 3 in the supplementary material. The thermal conductivity of a single crystalline KTF (1.6 W m^{-1} K^{-1})[13] is nearly an order of magnitude smaller than that of YAG (14 W m^{-1} K^{-1}), a disparity that can be partly explained by the difference in elastic moduli. The lattice thermal conductivity of a material (the dominant term in κ for insulators) is highly dependent on the phonon velocities in a material, which, in turn, are proportional to the square root of elastic stiffness.[47]

The average low-frequency acoustic phonon velocities (e.g., the speed of sound) can be calculated exactly from the elastic moduli[16,17] and are given for KTF (∼3000 m/s) and YAG (∼5450 m/s) in Table I. The lower speed of sound of KTF cannot fully explain the tenfold difference in thermal conductivity. The exceptionally low K of KTF might also be caused by the complexity of the KTF unit cell, compared with some of the simpler compounds in Fig. 3. The structure of KTb_3F_{10} contains two distinct structural units: Tb^{3+} is eightfold coordinated by F in (TbF_8) forming a square antiprism, while the larger K^+ cation is coordinated by 16 F atoms.[35] Isostructural AB_3F_{10} fluorides also contain large A cations such as Ba and Rb, which are necessary to stabilize the unusually large 16-fold coordination environment.[36,37]

Although low thermal conductivity is usually not desirable in optical components, there are advantages to optical materials with low elastic moduli. In particular, fluorides are favored in some applications because of their low phonon energies, which are often cited as the origin of their wide optical transparency range from the UV to the IR.[38–41] Measurements of the elastic moduli, although only providing *direct* information about low frequency acoustic phonons, can be used to estimate the Debye frequency and temperature (i.e., the energy of the highest frequency phonons). To investigate Θ_D of our YAG and KTF crystals, we have used the sound-velocity-determined Debye temperature equations listed in Section 4 in the supplementary material.[16,17] We found $\Theta_D = 360$ K and 719 K for the KTF and YAG crystals, respectively. To date, this is the first report on the Debye temperature for KTF crystals. The Debye temperature of our YAG sample evaluated by

using the average sound velocity was found to be within 4% of previously reported values ($\Theta_D = 750$ K).[46]

IV. SUMMARY

Resonant ultrasound spectroscopy was used to determine the three independent elastic moduli, C_{11}, C_{14}, and C_{12}, of high-quality single crystalline cubic laser materials, KTF and YAG. The temperature derivatives of the elastic moduli were also determined, which may be useful in future studies to extrapolate the moduli to working temperatures of interest. The obtained low average sound velocity, Young's modulus, and shear modulus suggest relatively weak bonding in KTF. This finding is consistent with a previous report of low thermal conductivity in KTF. Further, low speed of sound is associated with "soft phonons" and a low Debye temperature, which, in turn, may explain the excellent infrared transparency of KTF. For YAG, the experimental measurements are in agreement with previously published reports. In summary, we provide the first report of elastic moduli in KTF, as well as direct evidence to understand the origins of low thermal conductivity and high infrared transparency in this material.

SUPPLEMENTARY MATERIAL

See the supplementary material for ultrasonic measurement details and temperature-dependent RUS data analysis for elastic moduli of KTF and YAG single crystals.

ACKNOWLEDGMENTS

This research was supported by the U.S. Department of Energy (DOE), Office of Basic Energy Sciences, Division of Materials Sciences and Engineering under Award No. DE-SC0019252.

DATA AVAILABILITY

The data that support the findings of this study are available within the article and its supplementary material.

REFERENCES

[1]M. J. Weber, Proc. SPIE **0681**, 75–90 (1987).
[2]E. A. Khazanov, Usp. Fiz. Nauk J. **59**(9), 886–909 (2016).
[3]I. L. Snetkov, A. V. Voitovich, O. V. Palashov, and E. A. Khazanov, IEEE J. Quantum Electron. **50**(6), 434–443 (2014).
[4]R. Yasuhara, I. Snetkov, A. Starobor, D. Zheleznov, O. Palashov, E. Khazanov, H. Nozawa, and T. Yanagitani, Opt. Lett. **39**(5), 1145–1148 (2014).
[5]D. Zheleznov, A. Starobor, O. Palashov, C. Chen, and S. Zhou, Opt. Express **22**(3), 2578-–2583 (2014).
[6]H. Yoshida, K. Tsubakimoto, Y. Fujimoto, K. Mikami, H. Fujita, N. Miyanaga, H. Nozawa, H. Yagi, T. Yanagitani, Y. Nagata, and H. Kinoshita, Opt. Express **19**(16), 15181–15187 (2011).
[7]D. Vojna, O. Slezak, A. Lucianetti, and T. Mocek, Appl. Sci. **9**, 3160 (2019).
[8]A. V. Starobor and E. A. Mironov and O.V. Palashov, Opt. Mater. **98**, 109469 (2019).
[9]K. T. Stevens, W. Schlichting, G. Foundos, A. Payne, and E. Rogers, Laser Technik J. **13**(3), 18–21 (2016).
[10]M. J. Weber, R. Morgret, S. Y. Leung, J. A. Griffin, D. Gabbe, and A. Linz, J. Appl. Phys. **49**, 3464–3469 (1978).
[11]D. Vojna, M. Duda, R. Yasuhara, O. Slez'ak, W. Schlichting, K. Stevens, H. Chen, A. Lucianetti, and T. Mocek, Opt. Lett. **45**(7), 1683–1686 (2020).
[12]J. A. Griffin, J. Folkins, M. J. Weber, R. Morgret, J. D. Litster, D. Gabbe, and A. Linz, J. Appl. Phys. **49**, 2209 (1978).
[13]A. A. Jalali, E. Rogers, and K. Stevens, Opt. Lett. **42**(5), 899–902 (2017).
[14]W. Schlichting, K. Stevens, G. Foundos, and A. Payne, Proc. OPTIFAB **2017**, 104481N (2017).
[15]H. M. Ledbetter and E. R. Naimon, J. Appl. Phys. **45**, 66 (1974).
[16]O. L. Anderson, J. Phys. Chem. Solids **12**, 41–52 (1959).
[17]O. L. Anderson, J. Phys. Chem. Solids **24**, 909–917 (1963).
[18]M. de Jong, W. Chen, T. Angsten, A. Jain, R. Notestine, A. Gamst, M. Sluiter, C. K. Ande, S. V. D. Zwaag, J. J. Plata, C. Toher, S. Curtarolo, G. Ceder, K. A. Persson, and M. Asta, Sci. Data **2**, 150009 (2015).
[19]T. S. Duffy, Am. Mineral. **103**, 977–988 (2018).
[20]P. R. Stoddart, P. E. Ngoepe, P. M. Mjwara, J. D. Comins, and G. A. Saunders, J. Appl. Phys. **73**, 7298–7301 (1993).
[21]G. A. Saunders, S. C. Parker, N. Benbattouche, and H. L. Alberts, Phys. Rev. B **46**, 8756–8767 (1992).
[22]W. J. Alton and A. J. Barlow, J. Appl. Phys. **38**, 3023–3024 (1967).
[23]V. F. Kitaeva, E. V. Zharikov, and I. L. Chistyi, Phys. Stat. Sol. (a) **92**(2), 475–488 (1985).
[24]R. G. Leisure and F. A. Willis, J. Phys. Condens. Matter **9**(28), 6001–6029 (1997).
[25]A. Migliori and J. D. Maynard, Rev. Sci. Instrum. **76**(16), 121301 (2005).
[26]F. F. Balakirev, S. M. Ennaceur, R. J. Migliori, B. Maiorov, and A. Migliori, Rev. Sci. Instrum. **90**(12), 121401 (2019).
[27]M. Born, J. Chem. Phys. **7**(8), 591 (1939).
[28]J. K. D. Verma and B. D. Nag, J. Phys. Soc. Jpn. **20**, 635–636 (1965).
[29]W. Voigt, *Lehrbuch der Kristallphysik* (Teubner, Berlin, 1910).
[30]A. Reuss, Z. Angew. Math. Mech. **9**, 49 (1929).
[31]J. Chen, L. Li, T. Yu, H. Long, D. Weidner, L. Wang, and M. Vaughan, J. Phys. Condens. Matter **18**(25), S1049 (2006).
[32]S. F. Pugh, Philos. Mag. **45**, 823–843 (2009).
[33]Y. P. Varshni, Phys. Rev. B **2**(10), 3952–3958 (1970).
[34]Y. Suzuki, J. B. Levine, A. Migliori, J. D. Garrett, R. B. Kaner, V. R. Fanelli, and J. B. Betts, J. Acoust. Soc. Am. **127**, 2797 (2010).
[35]N. V. Podberezskaya, O. G. Potapova, S. V. Borisov, and Y. V. Gatilov, J. Struct. Chem. **17**, 815–817 (1976).
[36]A. P. Ayala, M. A. S. Oliveiray, J. Y. Geslandz, and R. L. Moreiray, J. Phys. Condens. Matter **10**, 5161–5170 (1998).
[37]S. Matar, J. M. Reau, G. Villeneuve, J. L. Soubeyroux, and P. Hagenmuller, Radiat. Eff. **75**, 55 (1983).
[38]L. Jeffrey, A. Therton, and S. A. Payne, Annu. Rev. Mater. Sci. **23**(1), 453–502 (1993).
[39]A. J. Stevenson, H. Serier-Brault, P. Gredin, and M. Mortier, J. Fluor. Chem. **132**, 1165–1173 (2011).
[40]S. M. Lima, T. Catunda, R. Lebullenger, A. C. Hernandes, M. L. Baesso, A. C. Bento, and L. C. M. Miranda, Phys. Rev. B **60**(22), 15173 (1999).
[41]M. Poulain, M. Poulain, and M. Matecki, J. Non-Cryst. Solids **51**, 201–215 (1982).
[42]P. Blanchfield and G. A. Saunders, J. Phys. C Solid State Phys. **12**(22), 4673–4689 (1979).
[43]A. J. H. Mante and J. Volger, Phys. Lett. **24A**(3), 139–140 (1967).
[44]Y. Fu and D. J. Singh, Phys. Rev. Mater. **2**, 094408 (2018).
[45]B. Schulz and M. Hoffmann, High Temp. High Pressures **34**, 203–212 (2002).
[46]J. F. W. Gunsser and U. Wolfmeier, "Debye temperature," in *Magnetic and Other Properties of Oxides and Related Compounds. Part A: Garnets and Perovskites*, edited by K.-H. Hellwege and A. M. Hellwege (Springer-Verlag, 1978), Vol. 12A.
[47]E. S. Toberer, A. Zevalkink, and G. J. Snyder, J. Mater. Chem. **21**, 15843–15852 (2011).